An approximated Snake Function for Road Extraction from digital images

Leila Mohammadnia[1] and Jalal Amini[2]

[1] Kharazmi Research, Pakdasht, Iran

Email: lmohamadnia@gmail.com

[2]Department of geomantic engineering, collage of Engineering, University of Tehran, Tehran, Iran

Email: jamini@ut.ac.ir

ABSTRACT

This paper proposes an optimized mathematical model (Snake-ant) for linear feature extraction from satellite images. The model first uses the Ant Colony Optimization (ACO) to establish a pheromone matrix that represents the pheromone information at each pixel position of the image, according to the movements of a number of ants which are sent to move on the image. Next pheromone matrix is used in the snake model as external energy to extract the linear features like roads edges in image. Snake is a parametric curve which is allowed to deform from some arbitrary initial location toward the desired final location by minimizing an energy function based on the internal and external energy. Our approach is validated by a series of tests on satellite images.

Keywords

ant colony optimization; image edge detection; road, **s**atellite image**;** Snake.

Council for Innovative Research

Peer Review Research Publishing System

1. INTRODUCTION

In the last years, many approaches developed to deal with detecting linear features on satellite images [1]–[10]. Snakes, also called Active Contour Models, were introduced by Kass [11], and are used for extracting linear features in images. Compared with other extraction methods for linear features, the main advantage of snakes is that geometric properties of the features can be embedded constraints and used directly to guide the search. in road extraction, snakes are applied to extraction of road sides and centerlines [12] - [14]. On the one side, geometric constraints corresponding to road properties such as connectivity, low curvature and constant width are incorporated into snakes. This invokes *internal forces* which force the snake to satisfy defined road properties. On the other side, the photometric constraints are used to specify relations between snakes and images. When snakes are for instance applied to extracting road sides, photometric constraints require image gradient magnitude to assume a local maximum along the curve of the snake. Photometric constraints invoke internal forces which push the snake toward contours of contrast in images. When internal and external forces are defined, road extraction is performed by optimizing the position of the snake. This paper proposes an improved approach based on the ant colony optimization algorithm to detect a matrix pheromone based on the routes formed by the ants sent on the image . Next pheromone matrix is used in the snake model as external energy to extract the roads edges.

At the rest of this paper, section 2 illustrates material and method. The experimental results will be given in section 3 and finally section 4presents the conclusions and remarks.

2. Material and method

2. 1 pheromone matrix extraction

The aim of the Ant Colony optimization is iteratively find the best solution of the problem through a guided search over the solution space, by constructing the pheromone information. Suppose totally K ants are applied to find the best solution in a space χ that consists of M1 × M2 nodes. There are two basic issues in the ACO process; that is, the probabilistic transition matrix $p^{(n)}$ and the update of the pheromone matrix $\tau^{(n)}$.

First, at the *n*-th construction-step of ACO, the *k*-th ant moves from the node *i* to the node *j* according to a probabilistic action rule, which is determined by [15]

$$p_{i,j}^{n} = \frac{\left(\tau_{i,j}^{(n-1)}\right)^{\alpha}\left(\eta_{i,j}\right)^{\beta}}{\sum_{j\in\sum\Omega_i}\left(\tau_{i,j}^{(n-1)}\right)^{\alpha}\left(\eta_{i,j}\right)^{\beta}} \quad if \quad j\in\Omega_i \tag{1}$$

Where $\tau_{i,j}^{n-1}$ is the pheromone information value of the arc linking the node *i* to the node *j*; Ω_i is the neighborhood nodes for the ant a_k given that it is on the node *i*; the constants α and β represent the influence of pheromone information and heuristic information, respectively; $\eta_{i,j}$ represents the heuristic information for going from node i to node j, which is fixed to be same for each construction-step.

Second, the pheromone matrix needs to be updated twice during the ACO procedure. The first update is performed after the movement of each ant within each construction step. To be more specific, after the move of the k-th ant in the n-th construction-step, the pheromone matrix is updated as [15]

$$\tau_{i,j}^{n-1} = \begin{cases} (1-\rho)\ \tau_{i,j}^{(n-1)} + \rho\,\Delta_{i,j}^{(k)} & if\ (i,j)\ belongs\ to\ the\ \ tour \\ \tau_{i,j}^{(n-1)} & otherwise \end{cases} \tag{2}$$

Where ρ is the evaporation rate. Furthermore, the determination of best tour is subject to the user-defined criterion, it could be either the best tour found in the current construction-step, or the best solution found since the start of the algorithm, or a combination of both of the above two. The second update is performed after the move of *all* K ants within each construction-step; and the pheromone matrix is updated as [15]

$$\tau^{(n)} = (1-\psi)\ \tau^{(n-1)} + \psi\ \tau^{(0)} \tag{3}$$

Where ψ is the pheromone decay coefficient .

The matrix pheromone extraction process is started from the initialization process by ants. Then the ants move more on the image to find the edges based on the edge characteristics. From the new locations of each ant, the process runs for N

iterations to construct the pheromone matrix by iteratively performing both the construction process and the update process. Finally, the decision process is performed to determine and identify the road edges.

For this process in detail, assume totally K ants are assigned on the image **I** with a size of M1 ×M2, each pixel of which can be viewed as a node. The initial value of each component of the pheromone matrix $\tau^{(0)}$ is set to be a constant. τ_{init}

At the *n*-th construction step, one ant is randomly selected from the above-mentioned total K ants, and this ant will consecutively move on the image for L movement steps. This ant moves from the node (*l*, *m*) to its neighboring node (*i*, *j*) according to a transition probability that is defined as

$$p^n_{(l,m),(i,j)} = \frac{\left(\tau^{(n-1)}_{i,j}\right)^\alpha \left(\eta_{i,j}\right)^\beta}{\sum\limits_{(i,j)\in\sum\Omega_{(l,m)}} \left(\tau^{(n-1)}_{i,j}\right)^\alpha \left(\eta_{i,j}\right)^\beta} \tag{4}$$

Where $\tau^{n-1}_{i,j}$ is the pheromone value of the node (i, j), $\Omega_{(l,m)}$ is the neighborhood nodes of the node (l, m), $\eta_{i,j}$ represents the heuristic information at the node (i, j).

There are two issues in the construction process. The first issue is determination the heuristic information $\eta_{i,j}$ in (4). In this paper, it is proposed to be determined by the local statistics at the pixel position (i, j) as

$$\eta_{i,j} = (I(i,j) - I_m(i,j))^2 \tag{5}$$

Where $I(i,j)$ is the intensity value of the pixel at the position (*i* , *j*) of the image **I**. $I_m(i,j)$ is the mean value of the intensity values of a window with size of 3×3 centered on (*i*, *j*).

The second issue is to determine the permissible range of the ant's movement in (4) at the position (*l*,*m*). In this paper, it is proposed to be either the 4-connectivity neighborhood or the 8-connectivity neighborhood, both of which are showed in Figure 1.
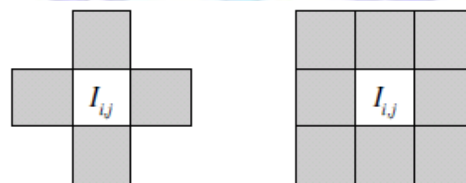

Figure 1.the ants movement in (a) 4-connectiving and (b) 8-connectiving

The proposed approach performs two updates operations for updating the pheromone matrix.

• The first update is performed after the movement of each ant within each construction-step. Each component of the pheromone matrix is updated according to

$$\tau^{n-1}_{i,j} = \begin{cases} (1-\rho)\ \tau^{(n-1)}_{i,j} + \rho\,\Delta^{(k)}_{i,j} & if\,(i,j)\ \ is\ visited\ by\,the\,current\ k-th\ ant \\ \tau^{(n-1)}_{i,j} & otherwise \end{cases} \tag{6}$$

Where ρ is defined in (2), $\Delta^{(k)}_{i,j}$ is determined by the heuristic matrix; that is, $\Delta^{(k)}_{i,j} = \eta_{i,j}$

• The second update is carried out after the movement of all ants within each construction-step according to

$$\tau^{(n)} = (1-\psi)\ \tau^{(n-1)} + \psi\ \tau^{(0)} \tag{7}$$

Where ψ is defined in (3).

Pheromone matrix is used in the snake model as external energy to extract the linear features like roads edges in image.

2.2 Road Vectors Extraction

Extraction of road edges is the last stage**.** The solution to be used is the snake approach .Snake is a parametric curve which is allowed to deform from some arbitrary initial location toward the desired final location by minimizing an energy function. In the continues domain, the snake is defined as a parametric curve, *r(s,t)* =(*x(s,t)*, *y(s,t)*), Where *s* is proportional

to arc length, *t* is the current time, and *x* and *y* are the curve's image coordinates[11]. The snake minimizes an energy function based on internal and external constraints at time *t*.

$$E_{tot}(r(s,t)) = \eta E_{int}(r(s,t)) + E_{ext}(r(s,t)) \tag{8}$$

Where E_{int} represents the *internal energy* of the snake due to bending, the external *energy* E_{ext} gives rise to the image forces. The position of the snake where all of its forces are compensated corresponds to the local minimum of the snake's total energy *E*. Thus the problem of the optimization of the snake's position is equivalent to the minimization of its energy.

The external energy of the snake can be defined as:

$$E_{ext}(\vec{v}) = -\int_0^1 p(\vec{v}(s,t)) \, ds \tag{9}$$

Where $p(\vec{v}(s,t))$ is a function with high values corresponding to the features of interest.

The internal energy makes it possible to introduce geometric constraints on the shape of the snake. It can be defined as:

$$E_{int}(\vec{v}) = \frac{1}{2}\int_0^1 \alpha(s)\frac{\partial \vec{v}(s,t)}{\partial s}^2 + \beta(s)\frac{\partial^2 \vec{v}(s,t)}{\partial s^2}^2 \, ds \tag{10}$$

where $\alpha(s)$ and $\beta(s)$ are arbitrary functions that regulate the snake's tension and rigidity. The constraint on tension is introduced by the first order term and makes the snake to act like a membrane. The rigidity is constrained by the second order term and makes the snake act like a thin plate.

the substitution of (9) and (10) into the equation of the snake's total energy (8) results in

$$E(\vec{v}) = -\int_0^1 p(\vec{v}(s,t)) \, ds + \frac{1}{2}\int_0^1 \alpha(s)\frac{\partial \vec{v}(s,t)}{\partial s}^2 + \beta(s)\frac{\partial^2 \vec{v}(s,t)}{\partial s^2}^2 \, ds \tag{11}$$

As shown in [16] if the snake minimizes the energy *E*, then according to the variational calculus in [17] it must be a solution to the *Euler-Lagrange* differential equation of motion

$$\frac{\partial}{\partial s}\left(\alpha(s)\frac{\partial \vec{v}(s,t)}{\partial s}\right) + \frac{\partial y}{\partial s^2}^2\left(\beta(s)\left(\frac{\partial^2 \vec{v}(s,t)}{\partial s^2}\right)\right) ds = -\nabla p(\vec{v}(s,t)) \tag{12}$$

By choosing a particular deformation energy in (10) the differential equation governing the motion of the snake becomes *linear*. This facilitates the numerical treatment of the minimization problem since (12) can be separated into two differential equations

$$\frac{\partial}{\partial s}\left(\alpha(s)\frac{\partial x(s,t)}{\partial s}\right) + \frac{\partial y}{\partial s^2}^2\left(\beta(s)\left(\frac{\partial^2 x(s,t)}{\partial s^2}\right)\right) ds = -\frac{\partial P}{\partial x} \tag{13}$$

$$\frac{\partial}{\partial s}\left(\alpha(s)\frac{\partial y(s,t)}{\partial s}\right) + \frac{\partial y}{\partial s^2}^2\left(\beta(s)\left(\frac{\partial^2 y(s,t)}{\partial s^2}\right)\right) ds = -\frac{\partial P}{\partial y} \tag{14}$$

and solved independently for *x(s, t)* and *y(s, t)*. However, in order for these equation to have a unique solution one must specify boundary conditions such as the values and derivatives of $x(s,t), y(s,t)$ for *s* = 0 and 1. Since in practice *P* is a discrete function, the equations (13),(14) cannot be solved analytically and require a numerical. Since the internal energy of the snake can be controlled, the balance can be achieved by the adjustment of functions $\alpha(s)$ and $\beta(s)$ which control the tension and rigidity of the snake.

As shown in [12] the balance between the internal and external energies can be effectively enforced by substitution of functions $\alpha(s)$ and $\beta(s)$ for a constant factor μ which value can be automatically calculated from

$$\mu = \left| \frac{\partial E_{img}(\vec{v})}{\partial E_{int}(\vec{v})} \right| \qquad (15)$$

where ∂ is the variational operator. The calculation is based on the assumption that the initial estimate of snake's position is close to the final solution. The optimization of the snake with automatically readjusted μ results in the stabilization of snake's position close to its previous one independently of the snake's shape and the image function. The substitution of $\alpha(s)$ and $\beta(s)$ with μ in (13),(14) results in equation

$$\mu\left(-\frac{\partial^2 v(s,t)}{\partial s^2} + \frac{\partial^4 v(s,t)}{\partial s^4} \right) = -\frac{\partial P}{\partial v} \qquad (16)$$

Where *v* stands either for *x* or *y*.

Solving equation (16) in a computer system implies that the evolution of the snake can be performed only in discrete time steps denoted further by [*t*]. In order to approximate the position and derivatives of the snake in (16), the discretization of the snake's representation is required, too. This can be achieved by sampling the snake at regular intervals into a polygonal curve with *n* vertices

$$\vec{v}^{[t]} = \left\{ \vec{v}_i^{[t]} \right\} =)\{ (x_i^{[t]}, y_i^{[t]}) = (x(i,t), x(i,t) \} \text{ for } i = 0, 1, \dots n-1 \qquad (17)$$

Then, taking the time step to be 1 the equation (16) can be rewritten in discrete form as

$$\mu(-(v_i^{[t]})_{ss} + (v_i^{[t]})_{ssss}) = -p_{v_i^{[t-1]}} \qquad (18)$$

where *v* stands either for *x* or *y* and $(v_i^{[t]})_{ss} \cdot (v_i^{[t]})_{ssss}$ denote the second and forth order derivatives of $v_i^{[t]}$ with respect to *s*. Note, that since (16) is an implicit equation the compromise is made to take the value of *P* into account at the old rather than at the new snake's position. Using central differences to approximate the derivatives $(v_i^{[t]})_{ss}$ and $(v_i^{[t]})_{ssss}$, the left hand side of (18) for vertices $v_i^{[t]}$, (*i* = 2, ..., *n* − 3) can be written as

$$\mu(-(v_i^{[t]})_{ss} + (v_i^{[t]})_{ssss}) \approx -\mu(v_{i-1}^{[t]} - 2v_i^{[t]} + v_{i+1}^{[t]}) + \mu(v_{i-2}^{[t]} - 4v_{i-1}^{[t]} + 6v_i^{[t]} - 4v_{i+1}^{[t]} + v_{i+2}^{[t]}) =$$
$$\mu(v_{i-2}^{[t]} - 5v_{i-1}^{[t]} + 8v_i^{[t]} - 5v_{i+1}^{[t]} + v_{i+2}^{[t]}) \qquad (19)$$

The set of equations for all vertices build a system that can be written in matrix form as

$$K.V^{[t]} = -P_{v^{[t-1]}} \qquad (20)$$

Where $V^{[t]}$ stands for either $(x_0^{[t]},...,x_{n-1}^{[t]})^T$ or $(y_0^{[t]},...,y_{n-1}^{[t]})^T$ and K is a symmetric n x n penta-diagonal matrix

$$K = \begin{bmatrix} 2\lambda & -3\lambda & \lambda \\ -3\lambda & 7\lambda & -5\lambda & \lambda \\ \lambda & -5\lambda & 8\lambda & -5\lambda & \lambda \\ & & & \cdot \\ & & & \cdot \\ & & & \cdot \\ & & \lambda & -5\lambda & 8\lambda & -5\lambda & \lambda \\ & & & \lambda & -5\lambda & 8\lambda & -5\lambda & \lambda \\ & & & & \lambda & -5\lambda & 7\lambda & -3\lambda \\ & & & & & \lambda & -3\lambda & 2\lambda \end{bmatrix} \tag{21}$$

However, as can be proven, the matrix K is singular and cannot be inverted. Thus, the equation (20) cannot be solved for $V^{[t]}$ directly. This corresponds to the noted above fact that differential equation (13),(14) must be supplied with 4 boundary values in order to have a unique solution. Such boundaries can be obtained for example by fixing two points and their tangent vectors at each end of the snake. However, in the original approach Kass use a friction force in order to constrain the displacement of the snake [11]. This is made by setting the right-hand side of equation

$$K.V^{[t]} + P_{v^{[t-1]}} = 0 \tag{22}$$

to the product of an iteration step (or a viscosity factor) γ and the negative time derivatives $(V^{[t-1]} - V^{[t]})$ .As result, the discrete equation of snake's motion can be written in the form

$$(K + \gamma I).V^{[t]} = \gamma V^{[t-1]} - P_{v^{[t-1]}} \tag{23}$$

Where **I** is an $n{\times}n$ identity matrix and $(K + \gamma I)$ is nonsingular and thus can be inverted. This implies that $V^{[t]}$ can be obtained directly by solving (23) numerically. As shown in Appendix A, the system of equations (23) can be effectively solved in $O(n)$ time with a fast method for inversion of the symmetric penta-diagonal matrix $(K + \gamma I)$. In order to find the position of the snake with local minimum of its energy the equation (23) is solved iteratively for a number of time steps. The iteration starts with the given initial position of the snake $V^{[0]}$. Following the viscosity γ can be computed according to [12]

$$\gamma = \frac{\sqrt{2n}}{\Delta} \left| \frac{\partial E(\vec{v})}{\partial \vec{v}} \right| \tag{24}$$

Where Δ is the permitted average displacement of the snake's vertices. The solution of (23) results in the new position of the snake for which its energy sum E is verified. The decrease of the energy in comparison to the previous time step indicates that the snake moves in the right direction toward the energy minima. Otherwise, if the energy has increased, the snake is kept at its previous position and the permitted displacement Δ is decreased. This continues until Δ becomes less than some threshold value. A small value for Δ indicates that the snake has been optimized to a position corresponding to the local minima of its energy.

3. Experimental Results

The proposed model applied to some satellite images. In the experiments, the fixed parameters were assigned values that found to produce good results. The parameters of the snake algorithm set as:

$\lambda = 5, \ \alpha = 2, \ \beta = 100$. And the parameters of the Ant colony algorithm set as:

$$\tau_{init} = .0001, \ N = 10, \ L = 40, \ K = 512, \ \alpha = 1, \ \beta = 1, \ \psi = .05, \ \rho = .1$$

The initial snake is generated by inserting nodes $\left[V^e\right]$ at regular distance intervals along the road segments. In this section, two examples with results will be given. First experimental is a part of image from a city (kish) in Iran as figure 2(a) and Road edges are shows in figure 2(b) after the snake-ant modeling.
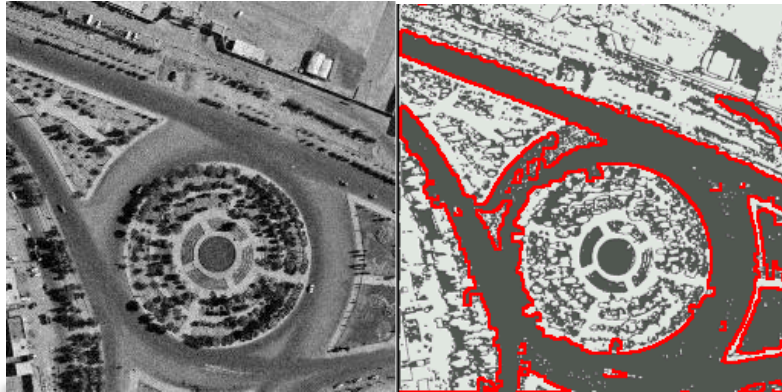
Figure2(a) original image (b)extracted road vector

Second experimental is also image taken from same area shown in figure 3(a) and Road edges are shows in figure 3(b) after the snake-Ant modeling.
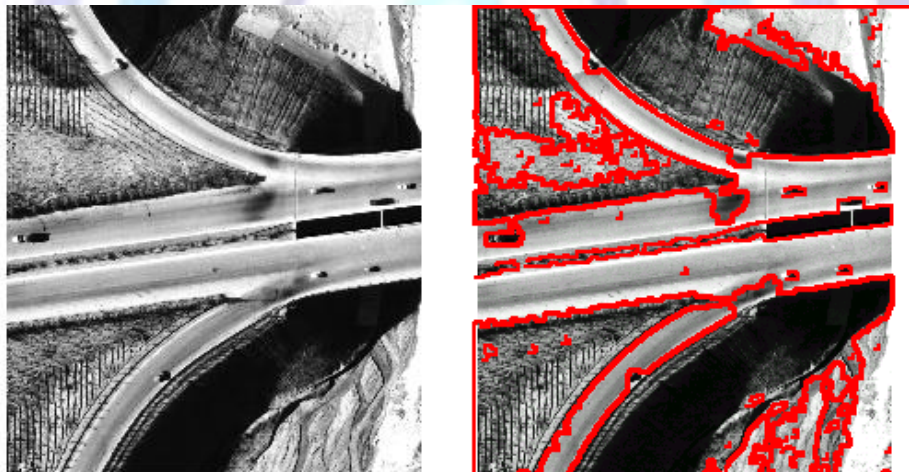

Figure3(a) original image (b)extracted road vector

For geometric accuracy assessment of the snake-Ant algorithm the road edges are extracted both manually as reference or ground-truth and automatically so that the accuracy of results could be assessed. To measure the impact of the restoration step, the snake localization process is achieved before and after restoration. Since the ground-truth is known, a quantification of the localization

Error is possible for both cases. Indeed, the obtained results are sampled and compared to the ground-truth vectors. This is achieved by measuring the average distance between the ground-truth and the obtained results as follows:

(25)

$$\overline{D} = \frac{1}{N_{sample}} \sum_{i=1}^{N_{ample}} \sqrt{(x_i - x_i^t)^2 + (y_i - y_i^t)^2}$$

Where (x_i, y_i) the coordinates of the obtained solution using the snake–Ant, and (x_i^t, y_i^t) are the coordinates of the ground-truth roads. Table 1 gives the obtained values for two examples.

2347-3487

ISSN: 2347-3487

Table 1.Average distance between the obtained solution and the ground –truth

	Experimental 1	Experimental 2
Width of road (Pixel)	0.68	1.07

The results showed that the proposed method is efficient in automatic linear feature extraction in **s**atellite images.

4. Conclusions

This paper developed a snake-ant model, for identifying and extracting linear feature such as road edges from the satellite images. The model was based on the improved ant colony model combined with the snake model to identifying and extracting the linear features from satellite images The ACO-based approach was able to establish a pheromone matrix that represents the pheromone information at each pixel position of the image. Next pheromone was used as the external energy in the snake model to extract the linear features like roads edges from images. The accuracy of the extracted road vectors was evaluated both visually and quantitavely. From viewpoint in visually, the extracted roads was close to the roads on the original image. From viewpoint in quantitavely, the statistical results confirmed that the proposed approach is also efficient .

5. REFERENCES

[1] F. Tupin, H. Maître, J. F. Mangin, J. M. Nicolas, and E. Pechersky, Detection of linear features in SAR images: Application to road network extraction, IEEE Trans. Geosci. Remote Sensing, vol. 36, Mar. (1998), pp. 434–452 .

[2] B. K. Jeon, J. J. Jang, and K. S. Hong, "Map-based road detection in spaceborne synthetic aperture radar images based on curvilinear structures extraction," Opt. Eng, vol. 39no. 9, (2000)

[3] J. Chanussot, G. Mauris, and P. Lambert, "Fuzzy fusion techniques for linear features detection in multitemporal SAR images," IEEE Trans. Geosci. Remote Sensing, vol. 37,(1999), pp. 1292–1305

[4] Y. Wang and Q. Zheng, "Recognition of roads and bridges in SAR images," Patt. Recognit., vol. 31, no. 7, (1998), pp. 965–977,

[5] M. F. Auclair-Fortier, D. Ziou, C. Armenakis, and S. Wang, "Automated correction and updating of road databases from high-resolution imagery," Can. J. Remote Sens., vol. 27, no. 1,Mar(2009), pp. 76–89

[6] H. Mayer, I. Laptev, A. Baumgartner, and C. Steger, "Automatic road extraction based on multi-scale modeling, context and snakes," Int. Arch. Photogramm. Remote Sens., pt. 3–2W3, vol. 32, Sept. (1997), pp. 106–113

[7] A. Baumgartner, C. T. Steger, H. Mayer, and W. Eckstein, "Multi-Resolution Semantic objects, and context for road extraction," in Semantic Modeling for the Acquisition of Topographic Information from Images and Maps, W. Fröstner and L. Plümer, Eds. Basel, Switzerland,(1997), pp. 140–156.

[8] N. Merlet and J. Zerubia, "Integration of Global Information for Roads Detection in Satellite Images," INRIA, 3239, 1997.

[9] C. Hivernat, X. Descombes, S. Randriamasy, and J. Zerubia, "Miseen Corespondance et Recalage de Graphes: Application aux Réseaux Routiers Extraits d'un Couple Carte/Image," INRIA, 3529, 1998.

[10] D. Klang, "Automatic detection of changes in road database using sattelite imagery," in Proc. Int. Archives Photogrammetry and Remote Sensing, vol. 32,(1998), pp. 293–298

[11] M. Kass, A. Witkin, and D. Terzopoulos, "Snakes: Active contour models," Int. J. Comput. Vis., vol. 1, no. 4, (1988), pp. 321–331

[12] Fua, P. and Leclerc, Y. Model Driven Edge Detection Machine Vision and

Applications, Vol. III, (1990).

[13] P. Trinder and Li, "Semi-Automatic Feature Extraction by Snake," Mach. Vis. Applicat.,

(1996)

[14] P. Neuenschwander, "From Ziplok Snakes to Velcro Surfaces," Mach. Vis. Applicat.,

(1996)

[15] M. Dorigo, M. Birattari, and T. Stutzle, "Ant colony optimization," IEEE Computational Intelligence Magazine, vol. 1, Nov (2006), pp. 28–39.

[16] Neuenschwander, W. Elastic Deformable Contour and Surface Models for 2-D and 3-D Image Segmentation, Hartung-Gorre Verlag, Konstanz(1996).

[17] Courant R. and Hilbert D. Methods of Mathematical Physics, volume 1. Wiley, NewYork (1989).

608 | P a g e   M a y 1 2 , 2 0 1 4

Leila Mohamadnia was born in kashmar, Iran, in 1978. she received the M.S. degree in applied mathematics ,numerical analysis from the Iran University of Science and Technology in 2007. She received the Ph. D . degree in applied mathematics ,numerical analysis from the Department of mathematic, Science and Research Branch, Islamic Azad University, Tehran, Iran in 2012. Her experience includes automatic object extraction (roads) from satellite images, Mathematic modelling of space images.

Jalal Amini was born in Mashhad, Iran, in 1969. He received the B.Sc. degree in surveying engineering from the K.N.Tossi University, Tehran, Iran, in 1993, the M.S. degree in photogrammetry from the K.N.Tossi University, Tehran, Iran, in 1996, and the Ph.D degree in photogrammetry and remote sensing from university of Tehran, Tehran, Iran, in 2001. He is currently as associate professor of remote sensing with the department of geomatics engineering, University of Tehran, Tehran, Iran. His experience includes automatic object extraction (roads) from satellite images, Mathematic modelling of space images, morphology, neural networks, fuzzy sets, fractals, DEM, classification, alpha-shapes, floodplain delineation, and microwave remote sensing including SAR signal processing.